

- Chang, S. J., Y. Li, M. Beauharnois, H. Huang, C. Lu, and G. Wojcik, 1996: *SARMAP Air Quality Model*. Atmospheric Science Research Center, University at Albany, State University of New York, 100 Fuller Road, Albany, New York 12205.
- Dennis, R. L., J. N. McHenry, W. R. Barchet, F. S. Binkowski, and D. W. Byun, 1993: Correcting RADM's surface underprediction: discovery and corrections of model errors and testing the corrections through comparisons against field data. *Atmospheric Environment*. 27A(60), 975-997.
- ERI, 1998: *Annual Progress Report of Connecticut Atmospheric Mercury Monitoring Network*. Environmental Research Institute, The University of Connecticut. Storrs, Connecticut.
- Fitzgerald, W. F., R. P. Mason, and G. M. Vandal, 1991: Atmospheric cycle and air-water exchange of mercury over mid-continental lacustrine regions. *Water, Air, and Soil Pollution*. 56, 745-767.
- Keeler, G., G. Glinsorn, and N. Pirrone, 1995: Particulate mercury in the atmosphere: its significance, transport, transformation and sources. *Water, Air, and Soil Pollution*. 80, 159-168.
- Keeler, G. J., and M. Hoyer, 1997: Recent measurements of atmospheric mercury in the Great Lakes region. pp305-321. In *Atmospheric Deposition of Contaminants to the Great Lakes and Coastal Waters*. Ed. J. E. Baker. SETAC Press. Pensacola, Florida.
- Northeast Regional Climate Center, 1997: *New England Climate*. 97(8). Ithaca, New York.
- Petersen, G., A. Iverfeldt, and J. Munthe, 1995: Atmospheric mercury species over central and northern Europe. Model calculations and comparison with observations from the Nordic Air and Precipitation Network for 1987 and 1988. *Atmospheric Environment*. 29(1), 47-67.
- Rea, A. W., G. J. Keeler, and T. Scherbatskoy, 1996: The deposition of mercury in throughfall and litterfall in the Lake Champlain watershed: a short term study. *Atmospheric Environment*. 30(19), 3257-3263.
- Seigneur C., Abeck H., Chia G., Reinhard M., Bloom N. S., Prestbo E., and Saxena P, 1998: Mercury adsorption to elemental carbon (soot) particles and atmospheric particulate matter. *Atmospheric Environment*. 32(14/15): 2649-2657.
- Tsai, Y., 1996: *Evaluation of two one-dimensional cloud models used in air quality models*. Thesis. Department of Atmospheric Science, University at Albany, State University of New York, 100 Fuller Road, Albany, New York 12205.
- USEPA, 1996: *Mercury study report to congress. Vol. II: An inventory of anthropogenic mercury emission in the United States*. Office of air quality Planning and Standards, Research Triangle park, NC, U.S.A.
- Xu, X., 1998: *A modeling study of regional scale atmospheric transport and transformation of mercury*. Ph.D. Dissertation. The University of Connecticut. Storrs, CT 06269.
- Xu X., Yang X., Miller D. R., Helble J. J., and Carley R. J, 1999: Formulation of bi-directional air-surface exchange of elemental mercury. *Atmospheric Environment*. 33(27), 4345-4355.

STRUCTURE OF PRIMARY PM_{2.5} DERIVED FROM DIESEL TRUCK EXHAUST

G. P. Huffman, F. E. Huggins, N. Shah and S. Pattanaik
University of Kentucky, CFELS, 111 Whalen Building,
533 S. Limestone St., Lexington, KY 40506

H. L. C. Meuzelaar and Sun Joo Jeon,
Department of Chemical & Fuels Engineering,
University of Utah, Salt Lake City, UT

D. Smith and B. Harris
U.S. Environmental Protection Agency, National Risk Management Res. Lab.,
Research Triangle Park, NC 27711

M. S. Seehra and A. Manivannan,
Physics Department, West Virginia University, Morgantown, WV

Key-Words: Particulate matter, PM_{2.5}, Diesel engine exhaust, thermal desorption GC/MS, XAFS spectroscopy, SQUID magnetometry

INTRODUCTION

The U.S. Environmental Protection Agency is currently considering regulations on airborne particulate matter < 2.5 microns in mean diameter (PM_{2.5}). It is important that the molecular structure and microstructure of PM_{2.5} from various sources be thoroughly characterized in order to identify structural features that may be important for source apportionment and health effects. Two of the primary sources of PM_{2.5} from petroleum are combustion of residual fuel oil and diesel engines. In previous papers, we have discussed the structure of PM_{2.5} derived from the combustion of residual fuel oil.^(1,2) In the current paper, we report some preliminary results on the molecular structure of primary PM_{2.5} from diesel vehicle tests. The techniques employed included thermal desorption (TD) GC/MS, x-ray absorption fine structure (XAFS) spectroscopy, and SQUID magnetometry.

SAMPLE GENERATION AND COLLECTION

The sample generation experiments were conducted by Harris and Smith at the EPA National Risk Management Research Laboratory (NRMRL). The samples were collected on teflon and quartz filters from the exhaust stack of a heavy-duty diesel truck. The total distance traveled by the truck during the sampling run was 191 miles at an average speed of 60.4 MPH. Diesel exhaust gas was sampled via a heated probe located two feet below the top of the exhaust stack. Hot exhaust gas passed through a PM_{2.5} cyclone and was subsequently cooled and diluted with ambient air. The average total stack gas exhaust rate over the duration of the sampling period was 15.5 Lpm. Four samples were collected simultaneously by establishing different gas flow rates to each of four filters, each 48 mm in diameter. This yielded two heavily loaded quartz filters (B and C, 6.2 mg of PM), one lightly loaded quartz filter (D, .5 mg of PM), and one lightly loaded Teflon (PTFE) filter (A, .6 mg of PM). Two additional filters (labeled PM1 and PM2) with intermediate loading (~2mg) were collected in a separate experiment.

ANALYTICAL CHARACTERIZATION

Thermal desorption GC/MS methodology

Filter strips (1.5 x 18 mm²) are positioned inside a special glass reaction tube that is lined with a ferromagnetic foil with a Curie temperature of 315°C. The tube is placed into a Curie-point reactor for desorption of volatile (VOC) and semivolatiles organic compounds (SVOC). In Curie-point desorption, a high frequency coil surrounds the glass tube and heats the foil by induction. The foil heats up till its Curie point is reached and its energy intake drops, thus holding the temperature of the foil at this point. Flash desorption of organic compounds from the particles immobilized by the filter strips is achieved using a total heating time of 10 s under a continuous flow of He carrier. The continuous flow of He transfers the analytes from the reaction zone into a fused silica capillary column of a gas chromatograph, coupled to a mass spectrometer. A more detailed description of the apparatus is given elsewhere.⁽³⁾

Conventional solvent-based extraction method has been used for extraction of soluble analytes from a more or less insoluble matrix. However, there are several practical problems with the application of solvent-based GC/MS techniques to ambient PM filter sample characterization,

compared to the TD method. Solvent-based GC/MS analysis of filter samples requires relatively large sample masses and the laboratory methods involved are laborious and use large quantities of solvents. Solvent extracts can include significant quantities of large soluble or even polymeric molecules that are unsuitable for direct GC/MS analysis but may contaminate the GC inlet.

The two heavily loaded quartz filters (B and C), produced qualitatively and quantitatively similar TD-GC/MS profiles. The data for sample B are shown in Figures 1 and 3. The TIC are marked by a strong *n*-butylbenzenesulfonamide peak, together with some of the ubiquitous alkylphthalate contaminants, notably dimethylphthalate. Hopanes and steranes are virtually absent.

Compared to the high flow samples B and C, the lightly loaded quartz fiber filter D produces approx. 40 % of the long chain alkane signal intensities and 25 % of the PAH intensities. Since the "total PM mass" of sample D should only be 10 % of samples B and C, there is an obvious nonlinear response within the five-step analytical procedure (i.e. sample collection + sample preservation during storage and transportation + filter subaliquotting + thermal desorption + GC/MS response).

The TIC of the lightly loaded Teflon (PTFE) filter sample A shows a drastic reduction in the first "hump", which represents an unresolved complex mixture, and an increase in the yield of the highly polar and labile *n*-alkanoic acids (Figure 2). Perhaps the most surprising finding is the strong even vs. odd predominance among the long chain alkanes (Figure 4). The opposite phenomenon (odd vs. even predominance) is well known among geochemical samples and is generally attributed to decarboxylation of biogenic fatty acids with even carbon numbers. A highly speculative interpretation could be that the even vs. odd *n*-alkane predominance shown by the PTFE filter desorbate is in fact the correct relative abundance for the particle-borne long chain alkanes, as is the even vs. odd *n*-alkanoic acid abundance. Both observations might be explained by synthetic, 2-carbon pathways in the soot formation process. During desorption of alkanolic acids from the quartz filter, however, a substantial amount of decarboxylation may occur, thereby turning the dominant, even carbon number, alkanolic acids into odd carbon number *n*-alkanes, thereby smoothing out the dips in the *n*-alkane distribution profile.

XAFS spectroscopy analysis

XAFS spectra were obtained at the S K-edge at beam line X-19A at the National Synchrotron Light Source (NSLS) and at the Cr, Fe, Ni and Zn K-edges at beam line 4-3 at the Stanford Synchrotron Radiation Laboratory (SSRL) and at beam line X-18B at NSLS. The concentrations of Fe and Zn (800 - 2000 ppm) were significantly higher than those of other metals in the samples and gave correspondingly better quality spectra. All spectra were collected in the fluorescent mode, using a Lytle detector for the sulfur spectra and a 13 element solid-state Ge detector for the metal spectra. Experimental procedures are described in detail elsewhere.^(4,5)

Figure 5 shows a typical S K-edge XANES spectrum, deconvoluted into its component peaks. The locations of the peaks are used to assign each feature to a particular molecular form of valence state of sulfur, as indicated by the labels in Figure 5. Then, using previously developed methodology,⁽⁴⁾ the areas under the various peaks can be converted into percentages of the total sulfur contained in each of the molecular forms or valence states identified. The results of this analysis for the diesel PM_{2.5} samples are summarized in Table 1. It is seen that sulfate is the dominant sulfur form, followed by a sulfone species (most probably the *n*-butylbenzene sulfonamide identified by TD/GC/MS), and a small amount of thiophenic sulfur.

Although the XAFS spectra of the metals were quite noisy given the small amount of material under irradiation, useful XANES spectra were obtained from iron and zinc. Whereas the iron XANES spectra appeared to be similar to ferric sulfate, the zinc XANES spectra were quite different from that of zinc sulfate. Chromium sulfate was identified in sample C2.

SQUID magnetometry

A SQUID magnetometer (Quantum Design Model MPMS) was used to measure the temperature variation of the magnetization, *M*, from 5 K to 350 K of several of the diesel PM_{2.5} samples. The data are corrected for the diamagnetic contribution (measured in separate experiments) from the filter and the polyethylene sample holder.

The variations observed for the samples PM1 and PM2 are nearly identical, both in magnitude as well as in temperature variation. In these cases, there is a rapid increase in *M* below 25 K, above which *M* is nearly temperature independent. For sample B, the rise in *M* at lower temperatures is spread over a larger temperature range, whereas for sample C, *M* is nearly temperature independent, with only a hint of an increase below 10 K.

The increase in M at lower temperatures can be described by the Curie-law $M = M_0 + CH/T$ where $C = N\mu^2/3k_B$ is the Curie constant, N is the concentration of impurities each with magnetic moment μ , and k_B is the Boltzmann constant.⁽⁶⁾ The plots of $(M - M_0)$ versus $1/T$ are linear below ~ 25 K for samples PM2, PM1 and B. Using $\mu = 1.7 \mu_B$ for spin $S = 1/2$ yields $N = 10, 5$ and 2 (in units of $10^{19}/g$) for PM2, PM1 and B, respectively. These levels of impurities have been observed from similar analysis in high purity activated carbon.⁽⁷⁾ The nature of these impurities including free radicals by low temperature electron spin resonance spectroscopy in the near future.

Acknowledgement: Support of this research under U.S. Department of Energy (FE/NPTO) contract No. DE-AC26-99BC15220 is gratefully acknowledged. The XAFS experiments were conducted at the Stanford Synchrotron Radiation Laboratory and the National Synchrotron Light Source, which are also supported by the U.S. DOE.

REFERENCES

1. G. P. Huffman, F. E. Huggins, N. Shah, R. Huggins, W. P. Linak, C. A. Miller, R. J. Pugmire, and H. L. C. Meuzelaar, *ACS Div. Fuel Chem. Preprints*, **45**(1), 6-10 (2000).
2. G. P. Huffman, F. E. Huggins, N. Shah, R. Huggins, W. P. Linak, C. A. Miller, R. J. Pugmire, H. L. C. Meuzelaar, M. Seehra, and A. Mannivannan, "Characterization of Fine Particulate Matter Produced by Combustion of Residual Fuel Oil," *J. Air & Waste Management Assoc.*, **50**, (2000), in the press.
3. Dworzanski, J.P.; McClennen, W.H.; Cole, P.A.; Thornton, S. N.; Arnold, N.S.; Snyder, A.P.; Meuzelaar, H.L.C., *Environ. Sci. Technol.*, **31**, 295-305 (1997).
4. G.P. Huffman, S. Mitra, F.E. Huggins, N. Shah, S.Vaidya, and F. Lu, *Energy & Fuels*, **5**, 574-581 (1991).
5. F.E. Huggins, N. Shah, J. Zhao, F. Lu, and G.P. Huffman, *Energy & Fuels*, **7**, 482-489 (1993).
6. V. S. Babu, L. Farinash and M. S. Seehra, *J. Mater. Res.*, **10**, 1075 (1995).
7. A. Manivannan, M. Chirila, N. C. Giles and M. S. Seehra, *Carbon*, **37**, 1741 (1999).

Table 1: Sulfur forms in diesel PM samples

Sample	Elemental S	Thiophene	Sulfone*	Sulfate
Diesel Filter PM1	< 1	3	7	90
Diesel Filter PM2	< 1	6	8	86
Diesel B2 9/99	< 1	< 1	2	98
Diesel C2 9/99	< 1	5	11	84

*Probably n-butylbenzenesulfonylformamide contaminant (see text)

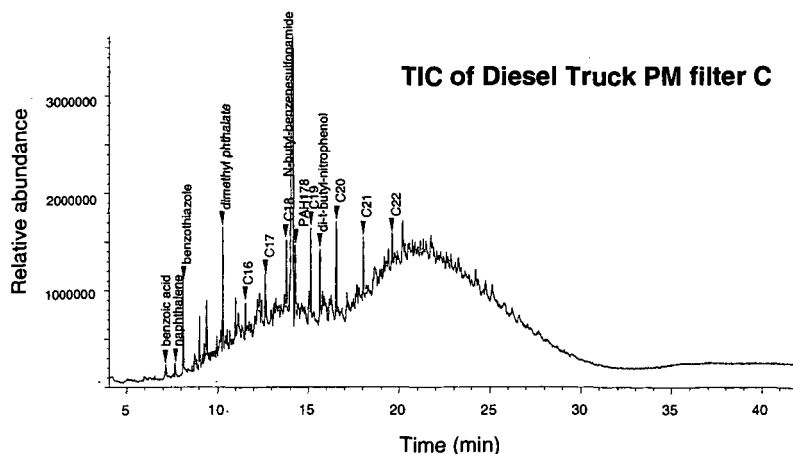


Figure 1: TIC of a heavily loaded diesel exhaust PM_{2.5} filter.

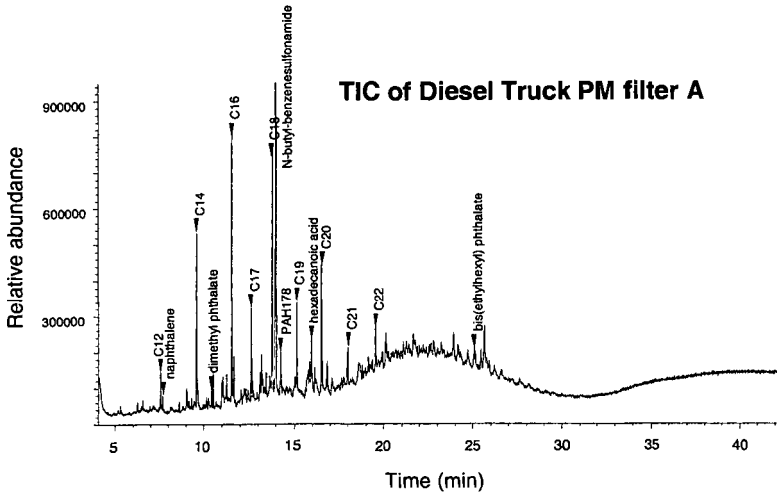


Figure 2. TIC of a lightly loaded diesel exhaust PM_{2.5} filter.

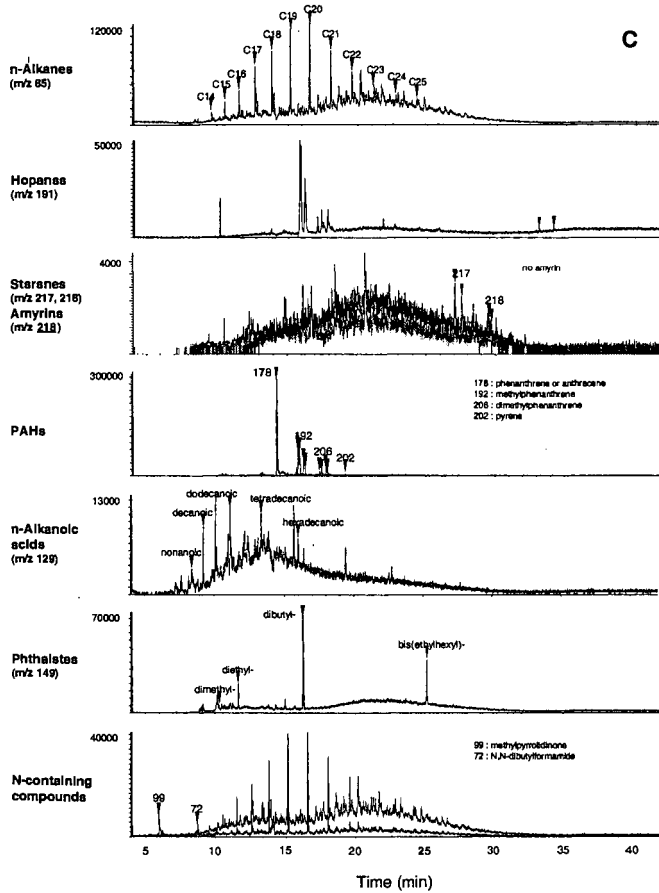


Figure 3: MS data for heavily loaded diesel exhaust PM_{2.5} filter sample B

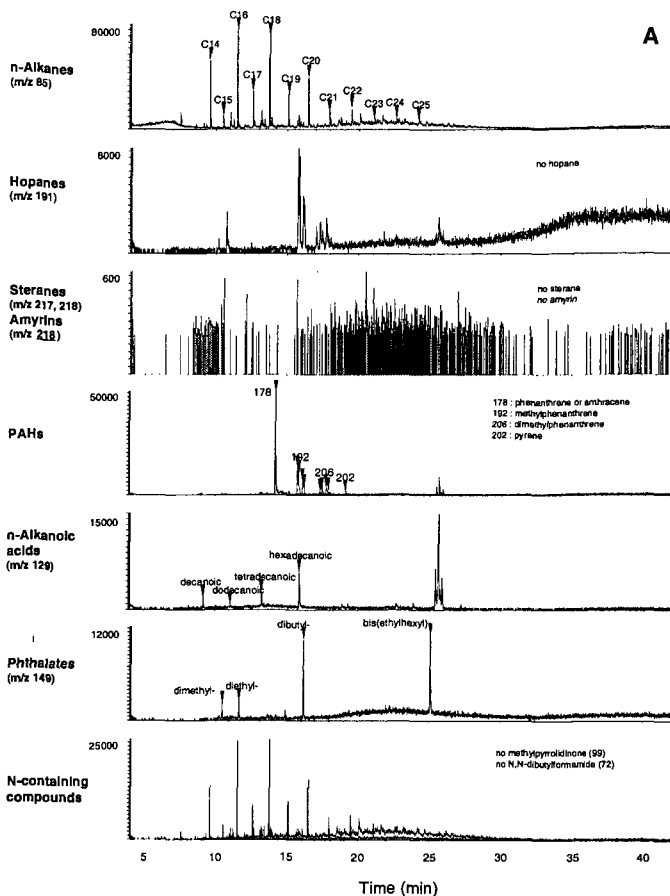


Figure 4. MS data for lightly loaded diesel exhaust PM_{2.5} filter sample.

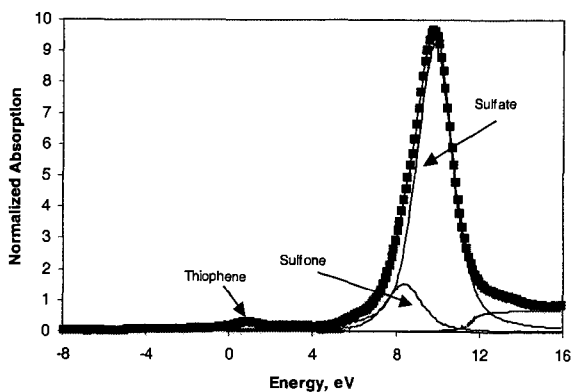


Figure 5: Least-squares fitted Sulfur K-edge XANES spectrum of Diesel PM sample "C2". The sulfone component is probably due to the n-butylbenzenesulfonamide contamination (see test).